Mixing in stratified-shear flows forced by internal waves

Cynthia E. Bluteau[1], Nicole L. Jones and Gregory N. Ivey

School of Civil, Environmental and Mining Engineering and the UWA Oceans Institute,
The University of Western Australia
35 Stirling Highway, Crawley, Australia, 6009
cynthia.bluteau@uwa.edu.au, nicole.jones@uwa.edu.au, greg.ivey@uwa.edu.au

Abstract

We present mixing observations from the Australian North West Shelf, where large semidiurnal tides, and shoaling nonlinear internal waves are generated offshore at the shelf-break. Around 30 moorings were deployed for about three weeks in April 2012 over several hundreds of kilometres, clustered around four nodes. We focus here on the near-bed turbulence and mean observations collected from one of the nodes where a 35-m long mooring (BUBS) was deployed in 105 m of water. The BUBS mooring was instrumented with mean velocity, temperature and conductivity sensors to derive the local mean shear S and stratification N. Turbulence observations were also obtained from more than 300 vertical microstructure shear profiles (VMP-500, Rockland Scientific) collected across the region. Our goal was to determine the intensity of the mixing, particularly during the passage of nonlinear internal waves, and to ultimately assess various mixing models.

1 Introduction

In the stratified-ocean, internal tides emanate from topographical features following the interaction of surface tides with local topography. Internal tides propagate over large distances before dissipating energy and are considered a major contributor to the global ocean energy budget (e.g., Wunsch et al., 2004). Accurately predicting mixing affects our ability to forecast global ocean circulation, and consequently climate change, given the coupling between the atmosphere and the ocean. Most mixing relationships used in environmental flows can be rewritten in the form of Richardson's 4/3 mixing law, which relates the turbulent kinetic energy dissipation ϵ and the size of large turbulent overturns L to the mixing rate K via $K \sim \epsilon^{1/3} L^{4/3}$. For instance, from the Osborn (1980) model $K_O = (R_f/(1-R_f))\,\epsilon/N^2$, if one assumes the flux Richardson number is constant at $R_f = 0.17$, this implies the mixing is controlled by the Ozmidov length scale $L_O = \sqrt{\epsilon/N^3}$. We recently demonstrated that mixing is controlled by the length-scale $L_\rho = f(\chi_T, S, N)$ (Ivey et al, JFM in prep.). This definition for L results in $K_\rho = \epsilon^{1/3} L_\rho^{4/3}$ and is consistent with the Osborn-Cox model:

$$K_T = \frac{1}{2}\frac{\chi_T}{T_Z^2} \tag{1}$$

where χ_T represents the dissipation of thermal variance and T_Z is the background vertical temperature gradient (Osborn and Cox, 1972). Equation 1 requires that temperature is the main contributor to stratification. These relationships also highlight the dependency of R_f on χ_T, ϵ and N. Here, we will demonstrate the intensity of mixing resulting from the passage of nonlinear internal waves on the Australian North West Shelf.

[1]Corresponding and Presenting Author

2 Methods

For three weeks in April 2012, the 35-m long BUBS mooring was deployed at the 105 m isobath (Figure 1a). BUBS was instrumented with two moored turbulence packages (MTP) at 7.5 and 20.5 m ASB. These high-frequency turbulence measurements (8 Hz) provide estimates of ϵ and χ_T via their respective inertial subranges (not shown here). The mooring was also instrumented with mean velocity, temperature and conductivity sensors to derive the local mean shear S and stratification N. Barotropic velocities were derived from the through water-column mooring located 200 m away in 100 m of water. This mooring was maintained by Australia's Integrated Marine Observation System (IMOS) and its data is publicly available at their website.

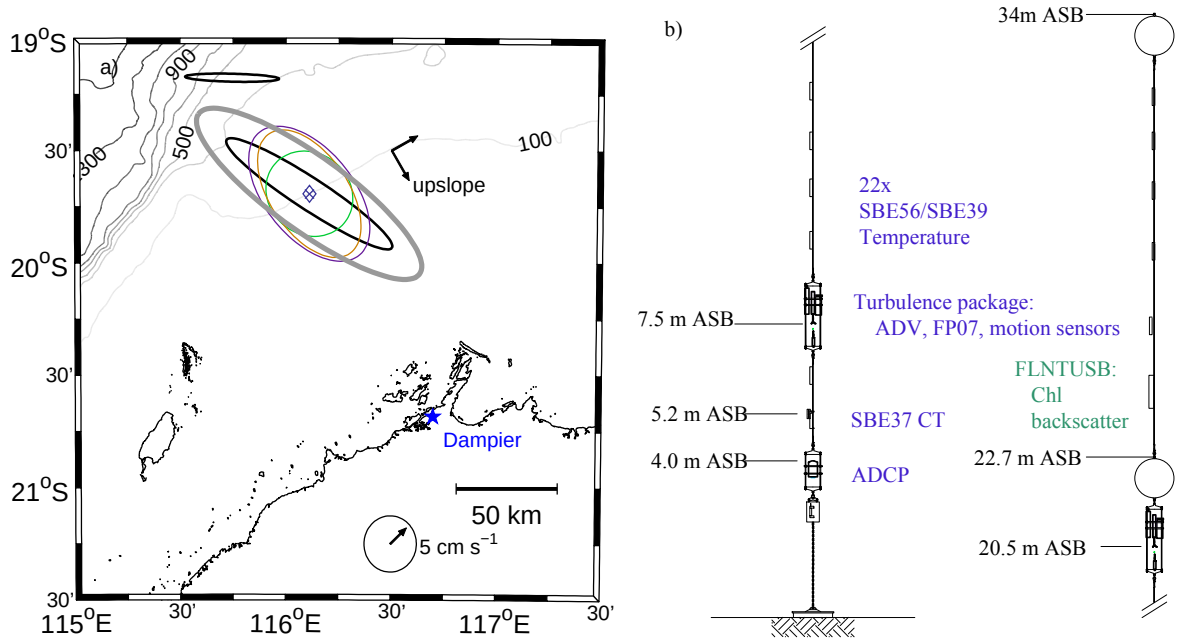

Figure 1: (a) Regional bathymetry with the location of BUBS mooring (diamond), and the IMOS mooring (X), and topographic up-slope direction indicated. (b) Schematic of the BUBS mooring with instrumentation. The principal component ellipses are derived from the observed IMOS mooring velocity: M2 barotropic ellipse (black). Baroclinic ellipses at 10 m ASB (purple), 38 m ASB (green), and 84 m ASB (orange). Depth-averaged total ellipse (gray).

Nearby the BUBS mooring, we collected 121 velocity shear profiles with a VMP500 (Rockland Scientific Ltd.) during a 24 h period starting at 0700 UTC 10 April 2012. The VMP recorded the velocity shear from two airfoil probes, in addition to information from the following sensors: 3-D accelerometers, a pressure sensor, high-accuracy temperature and conductivity sensors (SBE-3F and SBE-4C from Seabird Electronics) and a fast-response temperature sensor (FP07). All data channels sampled at 512 Hz. The VMP dissipation estimates ϵ were determined from the velocity shear spectra using two separate methods, which were assessed by Bluteau et al. (2016). We then used ϵ to estimate χ_T from the inertial-convective subrange of the temperature gradient spectra. Overall, the VMP provided profiles of ϵ, χ_T along with the vertical background density and temperature gradients necessary to estimate K_T.

3 Results

3.1 Background forcing

During the three-week deployment, the moored ADCP measured total currents as high as 0.8 m s^{-1} that propagated on average at -27° from due east, almost aligning with the topographic slope at -60° from due east (Figure 1a). The main tidal constituents represented in the recorded velocities and pressure at the BUBS mooring site are M2, S2, K1 and O1, with the semidiurnal components dominating the diurnal constituents (Table 1). Tidal amplitudes and velocities during spring tides exceeded 1.75 m and 0.5 m s^{-1}, respectively (Figure 2a). The magnitude of the major axis obtained via principal component analysis of the total depth-averaged velocities measured at the IMOS mooring was ≈0.25 m s^{-1}. This axis was aligned with the major axis of the M2 barotropic tide, but its magnitude was significantly larger (Figure 1a). A net along-isobath flow towards the south-west was observed over the three week period. Internal waves are generated offshore at the shelf-break (Bluteau et al., 2011). Their arrival at the site was not phase-locked with the barotropic tide (Figure 2 a-b). Baroclinic velocities associated with the passage of internal waves were largest near the seabed (Figure 2 c-g). The principal direction of propagation was more aligned with the topographic slope than the M2 barotropic ellipses (Figure 1a). The baroclinic velocity ellipses were more circular mid-depth, consistent with mode 1 internal waves (Figure 1a). The background stratification derived from the moored thermistors was nearly linear with a buoyancy period of about 9 minutes ($N \approx 1{\times}10^{-3}$ rad s^{-1}). The combination of the local topography, background stratification and large semidiurnal tides resulted in shoaling nonlinear internal waves that propagated through our site (Figure 2).

Table 1: Tidal elevation amplitudes and phases from the pressure measurements at the BUBS mooring site. Phases are relative to UTC.

Tidal constituent	**Amplitude**	**Amplitude error**	**Phase**	**Phase error**
	m	m	deg	deg
O1	0.14	0.02	166	11
K1	0.19	0.03	152	7
M2	0.80	0.08	66	6
S2	0.46	0.09	110	9

3.2 Mixing observations

The 24 h period of microstructure profiling occurred at the end of spring tides and coincided with the passage of two tidally-forced internal waves (Fig 2). The first packet of nonlinear internal waves passed the mooring site at around 1400 UTC at maximum flood tide. It was associated with a pulse of cold water and a sudden increase in the measured baroclinic velocities, especially near the seabed (Figure 2c). The estimated ϵ increased above 10^{-6} W kg^{-1} and then subsided over the next hour by nearly three orders of magnitude following the passage of the internal wave (Figure 2h). Mixing rates K_T were high, exceeding 10^{-3} m^2 s^{-1}. In contrast, the near-bed velocities associated with the second internal wave, shortly after 0300 UTC, were not as dramatic, although ϵ increased to 10^{-6} W kg^{-1} and persisted until 0400 UTC. The estimated mixing rates K_T varied over several orders of magnitude over the water column, and thus were much more variable

than when the first internal wave passed the site (Figure 2j). Osborn's model K_O with a constant Ri_f under-predicted mixing throughout the water column during the passage of the first internal wave (Bluteau et al., in prep GRL). The flux Richardson number derived Ri_f from the MTP was not constant, varying between 0.05 to 0.3 (not shown). Overall, the internal waves generated periods of intense mixing that was both time- and depth-dependent, which also varied with each internal wave.

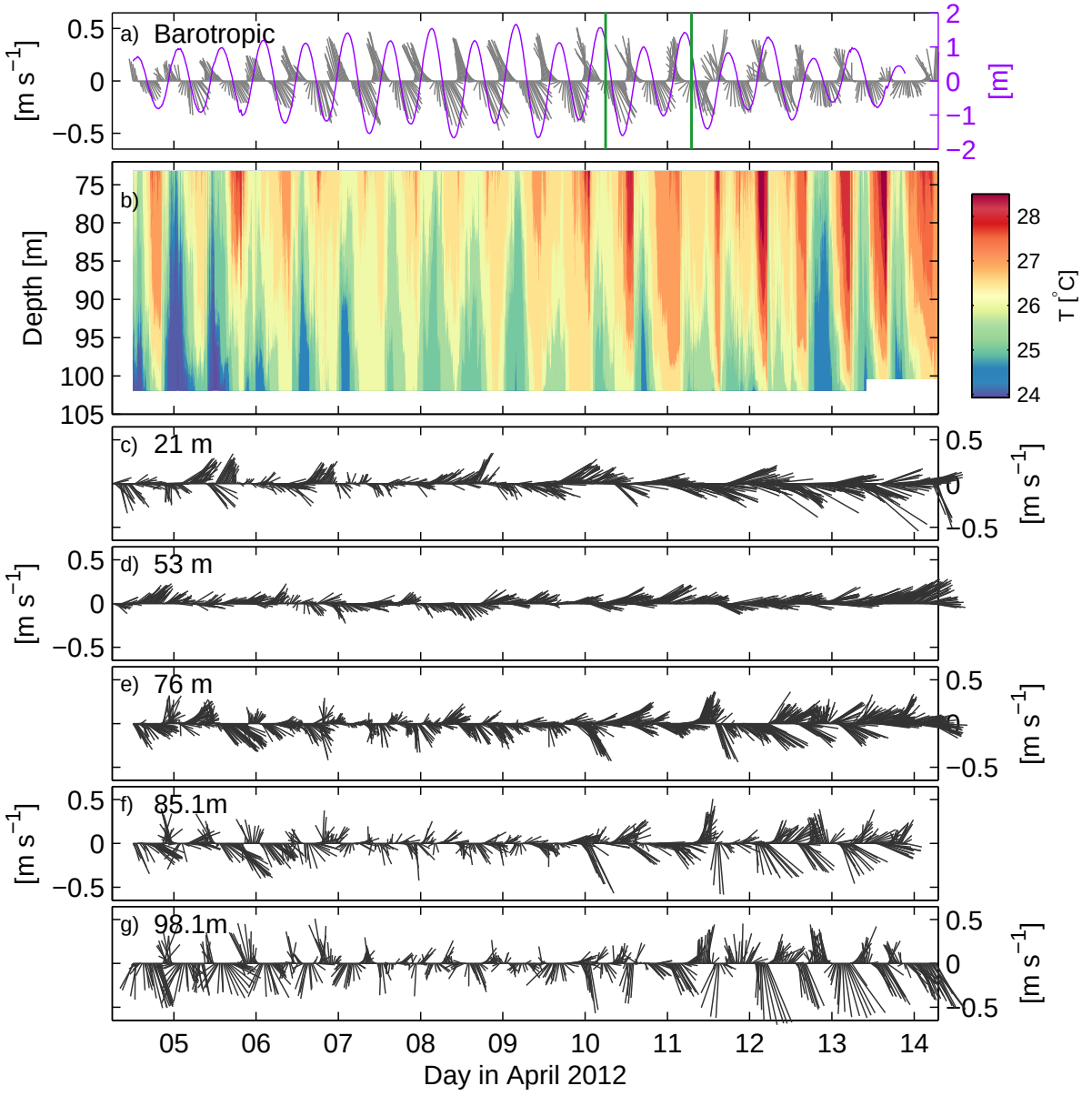

Figure 2: Observations at the BUBS site. a) Barotropic velocities and tidal elevations (from IMOS mooring). (b) Temperature contours from BUBS. (c-g) Baroclinic velocities at the labelled depth below the surface (from IMOS mooring). Green vertical lines in panel (a) denotes the 24-h period of VMP profiling shown in Figure 3.

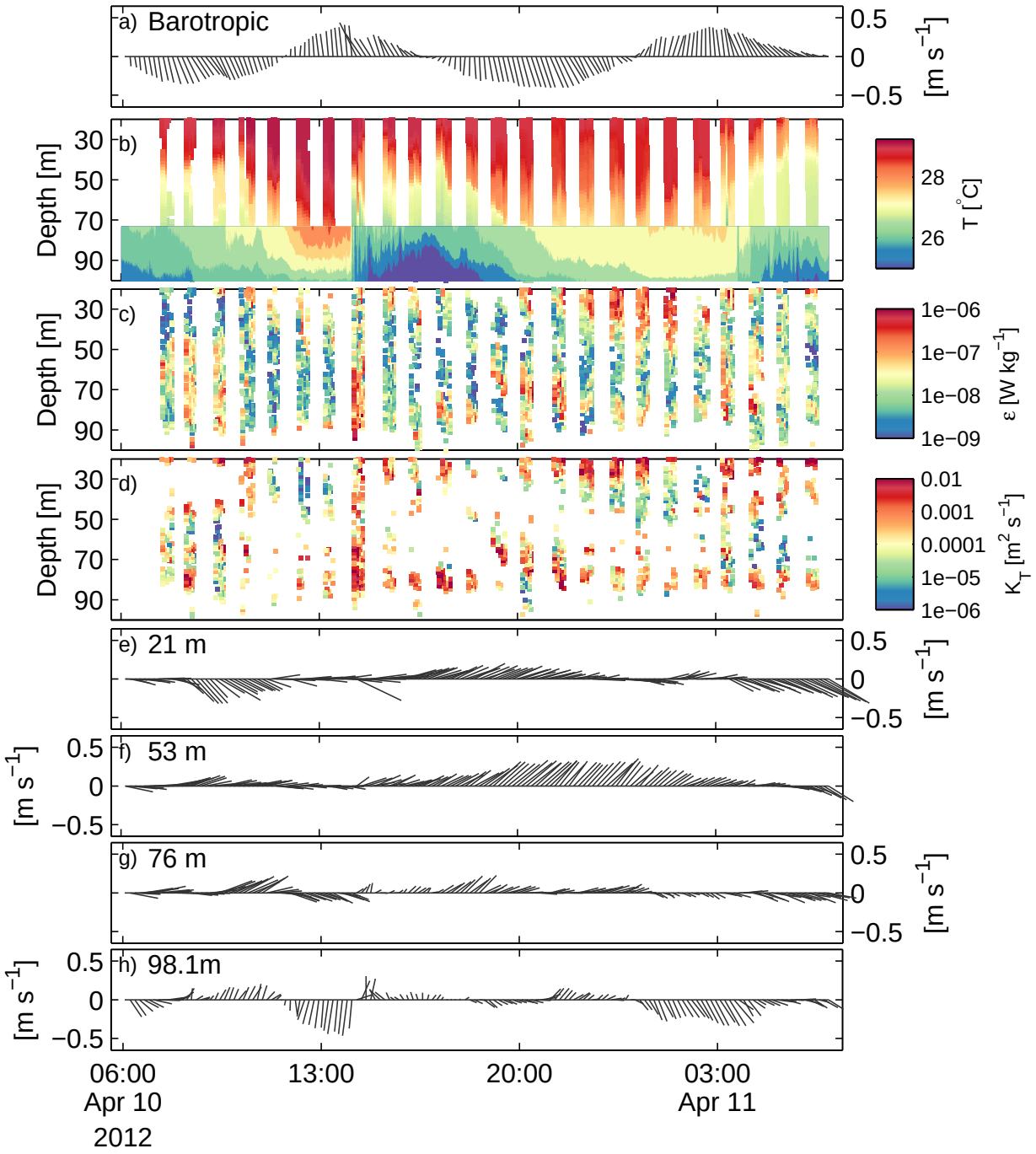

Figure 3: Observations at the BUBS mooring site over the 24-h period of VMP profiling. a) 10-min time-averaged barotropic velocities derived from the IMOS mooring. (b) Temperature recorded by the SBE3F overlaid with the contours from the temperature measurements on the BUBS mooring. (c) ϵ estimated from the velocity shear spectral observations from the VMP (Bluteau et al., 2016). (d) K_T estimated from equation 1 using the time-averaged local depth-averaged temperature gradients. (e-h) Baroclinic velocities at the labelled depth below the surface.

4 Conclusions

We presented preliminary mixing analysis at a site forced by internal waves. Strong mixing occurs during the passage of internal waves, although the baroclinic velocities are much weaker during spring tides. Future work includes extending the analysis to other NWS sites where VMP profiles were taken. We will use our observations to adapt some recently developed theories (Ivey et al., in prep) to the turbulence observations collected near the seabed. Finally, we plan to determine the influence of mixing on the water quality parameters that were collected at the BUBS location.

Acknowledgements

Two Australian Research Council Discovery Projects (DP 120103036 and DP 140101322), an Australian Research Council Linkage Project (LP110100017) and an Office of Naval Research, Naval International Cooperative Opportunities Project (N62909-11-1-7058) funded this work. We thank people from the Australian Institute of Marine Science, the Naval Research Laboratory and the University of Western Australia who aided in the collection of the data and the crew of the RV Solander. We also thank Anouk Messen who helped in the initial analysis of the VMP profiler.

References

Bluteau, C. E., Jones, N. L., and Ivey, G. N. (2011). Dynamics of a tidally-forced stratified shear flow on the continental slope. *J. Geophys. Res.*, 116(C11017).

Bluteau, C. E., Jones, N. L., and Ivey, G. N. (2016). Estimating turbulent dissipation from microstructure shear measurements using maximum likelihood spectral fitting over the inertial and viscous subranges. *J. Atmos. Oceanic Technol.*, 116.

Osborn, T. R. (1980). Estimates of the local rate of vertical diffusion from dissipation measurements. *J. Phys. Oceanogr.*, 10(1):83–89.

Osborn, T. R. and Cox, C. S. (1972). Oceanic fine structure. *Geophys. Fluid Dyn.*, 3(1):321–345.

Wunsch, C., , and Ferrari, R. (2004). Vertical mixing, energy, and the general circulation of the oceans. *Annu. Rev. Fluid Mech.*, 36(1):281–314.